(This is a sample cover image for this issue. The actual cover is not yet available at this time.)

Computers & Geosciences 54 (2013) 203–210

Contents lists available at SciVerse ScienceDirect

Computers & Geosciences

journal homepage: www.elsevier.com/locate/cageo

Mathematica code for least-squares cone fitting and equal-area stereonet representation

Kieran F. Mulchrone [a], Daniel Pastor-Galán [b,*], Gabriel Gutiérrez-Alonso [b]

[a] Department of Applied Mathematics, University College, Cork, Ireland
[b] Departamento de Geología, Universidad de Salamanca, 37008 Salamanca, Spain

ARTICLE INFO

Article history:
Received 15 October 2012
Received in revised form
23 January 2013
Accepted 24 January 2013
Available online 1 February 2013

Keywords:
Stereographic projection
Conical best fit
Complex conical shapes
Stereographic projection software
Stereogram plotting software

ABSTRACT

In structural geology it is often assumed that folds are cylindrical. However, most structures are conical to some degree. Due to the lack of software capable of accurately estimating the best fit cone from a set of oriented data, we developed a Mathematica application capable of (1) plotting oriented data (lines and planes) on an equal area stereonet, (2) calculating the orientation matrix, the distribution shape and intensity parameters, (3) plotting the eigenvectors and (4) estimating and plotting the best fit cone, a small circle. We present both synthetic and natural data demonstrating its robustness and accuracy calculating the best fit cone.

1. Introduction

Folds are cylindrical, most of them have, to a certain degree, a conical shape (Fig. 1). However, to our knowledge, the most popular free available stereographic applications such as Stereonet (Cardozo and Allmendinger, 2013; Allmendinger et al., 2012), Georient (Holcombe software), Openstereo (Grohmann and Campanha, 2010) or Stereo32 (Röller and Trepmann, 2008) or other Stereonet Mathematica applications – see Mathematica for Geology (Hanebergs) and Geological Program (Mookerjee) – either do not provide best fit cone functionality or provide methods which fail to estimate the best fit cone when dealing with complex distributions. In this paper we present Mathematica code which provides a robust cone fitting algorithm with the motivation of filling the gap found in other stereographic projection software.

A conical surface is the result of rotating an oblique line (the generator) around a defined rotation axis. In geology, geometrically, a conical fold is characterized by the trend and plunge of its axis and by the angle between the generatrix of the conical surface and the fold axis, also known as semiapical angle ($\alpha/2$) (Wilson, 1967; Pueyo et al., 2003). Perfect cylindrical folds can be considered as a special case of a conical fold; then have $\alpha/2$ equal to 0°. Identification and analysis of conical folds in nature are conducted using stereographic projection of geologic surfaces, typically bedding (π-diagrams) which, when truly representative of a conical surface, scatter along a small circle on the stereonet. When the geometry of the studied fold is more complicated, such as in elliptical conical folds or complex non-cylindrical folds, the π-diagram scatters along ellipses or irregular paths. Ramsay (1967 p. 349) indicated that conical folds are rare in nature, and (Ramsay and Huber, 1987, p. 311) suggested that the geometry of natural surfaces is probably more complex than a simple conical which is probably a more accurate assessment of the situation at most scales. Nevertheless, conical folding is often a valid approximation for non-cylindrical folds at suitably chosen scales and complex folded surfaces can be easily treated as several different conical surfaces.

Structural geologists have shown interest in conical folding trying to solve the problem of reconstructing bedding-parallel sedimentary lineation orientations (Cummins, 1966; Wilson, 1967; Ramsay, 1967 pp. 496–498) and, more recently, the problem of how to restore paleomagnetic data directions (Pueyo et al., 2003; Weil et al., 2013) or the location of mineralizations (Keppie et al., 2002) or hydrocarbon reservoir rocks (Mandujano and Keppie, 2006). The most frequently described conical geometry in rocks is the lateral terminations of cylindrical folds (e.g. Webb and Lawrence, 1986). The geometry is related to the propagation of folds during which both the interlimb tightening and fold axis lengthening occur. Moreover, conical folds can also form by fold interference (Ramsay, 1962; Wilson, 1967; Pastor-Galán et al., 2012a), or by folds forming in shear zones

* Corresponding author. Tel.: +34923294488.
E-mail address: dpastorgalan@usal.es (D. Pastor-Galán).

0098-3004/$ - see front matter © 2013 Elsevier Ltd. All rights reserved.
http://dx.doi.org/10.1016/j.cageo.2013.01.005

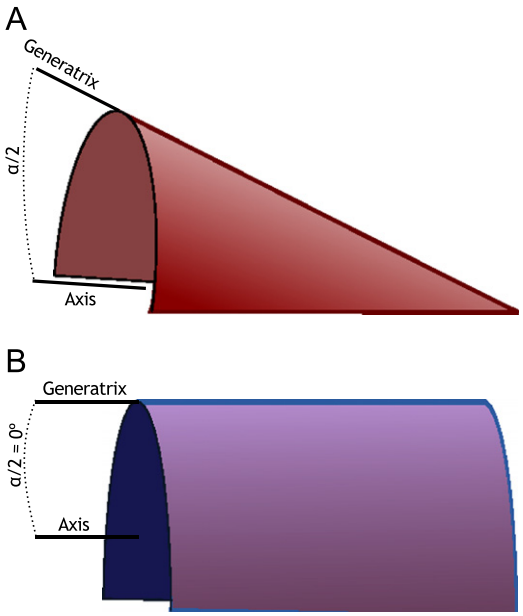

Fig. 1. Differences between a cylindrical and a conical fold.

(sheath-folds, e.g. Alsop and Carreras, 2007). Nicol (1993) demonstrated that surfaces formed by fold interference can be analysed as composite surfaces with segments displaying conical geometries. Furthermore, spatial variations in orientation of data and fold geometry may be related to the characteristics of the interfering fold pattern (Mulchrone, 1991; Nicol, 1993). Groshong (2008) emphasized the importance of distinguishing between cylindrical and conical folds because conical folds terminate along their axial trend.

Mathematical methods have been developed to fit measurements to a small circle and to quantify the suitability of the calculated fit (e.g. Ramsay, 1967; Fisher et al., 1987). Approaches to fitting planar data to a cone typically involve least squares minimisation of a function involving the direction cosines of poles to planes (Ramsay, 1967; Venkitasubramanyan, 1971; Cruden and Charlesworth, 1972), and provide estimates for the orientation of the cone axis and the semi-apical angle. Problems associated with these initial methods were resolved by minimising the squares of the actual angular deviations (Kelker and Langenberg, 1982; Fisher et al., 1987) by making the minimisation problem non-linear and requiring iterative techniques to determine a solution. The problem may also be solved using the least eigenvector of the orientation matrix (Fisher et al., 1987, p. 33), though this approach only works for symmetrical datasets with a semi-apical angle less than 45°. Bingham's distribution on a sphere can also be used to find the best-fit great circle to fold data forming a pair of clusters which is often the case for geological data (Kelker and Langenberg, 1976). Subsequently, using a transformation to spherical coordinates (Stockmal and Spang, 1982), a least-squares best fit was identified for the simulated data of Cruden and Charlesworth (1972). Methods able to cope with elliptical conical folds and statistical tests for distinguishing between circular and elliptical data have also been developed (Kelker and Langenberg, 1987, 1988). Non-geologists' statisticians have also shown an interest in this problem (Mardia and Gadsden, 1977; Rivest, 2008). We propose using an implementation of the iterative algorithm presented by (Fisher et al., 1987, p 140–143) that is based on the method of Mardia and Gadsden (1977) and the improved least-squares algorithm of Gray et al. (1980). This method is robust to apply to non-symmetrical data and has been proven to provide accurate solutions to different cases of real, as is the data used in this paper, and simulated conical folds. It works for non-symmetrical data and apical angles greater than 45°.

2. Code description and algorithms

The primary motivation for developing the code was to provide a robust cone fitting algorithm which was lacking in tested available software. Necessary additional functionality includes a collection of useful methods for analysis of orientation data typically collected by structural geologists. In this section a brief discussion and description of the data formats, analyses and graphical outputs are provided.

2.1. Plotting data

As far as the authors are aware, there is no internationally recognized standard for digital storage of oriented geological data. For this application data is stored in a text comma separated variable (csv) file format that can be readily imported into Mathematica and easily created in common spreadsheet packages such as Microsoft Excel, OpenOffice, etc. The file must conform to the following format: The first column contains either L (for linear data) or P (for planar data). If the data are planes then the next two columns contain either the strike and dip (using the right hand rule, Groshong, 2008, pp. 41–43; Ragan, 2009, p. 4) or dip direction and dip respectively. If the data are lines then the next two columns contain the trend and plunge respectively. The final and fourth column is reserved for categorization of data. Fig. 2 shows part of the contents of a data input file in Excel.

Once a file has been created it may be imported into Mathematica using the Import command. For convenience we provide a method, ImportSG, that simplifies the process. ImportSG takes two arguments: the first specifies the file to be imported and the second specifies the format used for planar data which may be either "RHR" (i.e. right hand rule strike and dip) or "DDD" (i.e. dip direction and dip data). ImportSG imports the data and separates it into subsets based on data type and category and also converts the orientation data into triplets of direction cosines, the format used in analysis and plotting routines. The data is subdivided into groups on the basis of whether it is planar of linear and also the category. For each unique combination of data-type and category a new group is created. This approach is unrestrictive but care needs to be taken when creating input files so that the resulting data is not too complex. It may be convenient to store files related to a single project in a single directory and rather than having to

	A	B	C	D	E	F	G
1	L	176	80	Overturned			
2	L	172	70	Overturned			
3	P	190	74	Overturned			
4	P	168	76	Overturned			
5	P	172	78	Overturned			
6	P	190	72	Overturned			
7	P	200	70	Overturned			
8	P	192	72	Overturned			
9	L	222	50	Normal			
10	L	215	57	Normal			
11	P	218	51	Normal			
12	P	220	53	Normal			
13	P	222	53	Normal			

inner_anticline

Fig. 2. Example format of data in excel. First column specifies if the data are planar or linear and the second column is the strike, dip direction or trend spending on the format. The third column specifies the dip or plunge and the final column is a category for analysis of complex datasets.

specify the full path to a file. The standard SetDirectory command can be used to select a particular directory for use.

The method EqualAreaPlot creates equal-area stereonets and has four arguments. The first argument is the data to be plotted and ought to be the output from ImportSG. The second argument specifies the size of the symbols on the stereonet and defaults to a value of 0.02. The third argument controls the colour and shape of the symbols used for each dataset in the data. For full control, a colour/shape combination for each dataset can be specified, otherwise, suitable values are randomly generated. The following shapes are provided: "Circle", an open circle, "FCircle", a filled circle, "OCircle", a filled circle with a black outline and similarly defined "Square", "FSquare", "OSquare". The final argument is either True or False and specifies whether or not a legend is displayed. The text of the legend is composed from the category and type of data. For example if the type is "L" and the category is "F1" then the legend is "F1 (L)". Example code:Click here to enter text.

```
(* select the directory with the data *)
SetDirectory["C:\\Users\\km\\Dropbox\\research papers\\ Conical Folding Mathematica\\Data"]
(* import data from csv file *)
data=ImportSG["inner_anticline.csv"];
(* create a plot of the data *)
EqualAreaPlot[data, 0.02, {{Purple,"Square"},{Blue,"OCircle"},
{Green,"OSquare"},{Red,"OCircle"}}, True]
```

The resulting plot is shown in Fig. 3. The code is fairly flexible and allows for a reasonable level of control to the user.

For less sophisticated data analysis, another more general SimpleEqualAreaPlot method is provided which takes four arguments. The first is a list of either strikes and dips or trends and plunges, the second specifies the type of data (either "P" or "L" respectively), the third determines the size of the symbol and the final argument specifies the type in the same way as for EqualAreaPlot above. Example code:Click here to enter text.

```
(* some data to be plotted *)
data = {{350,25},{120,56},{249,22}};
```

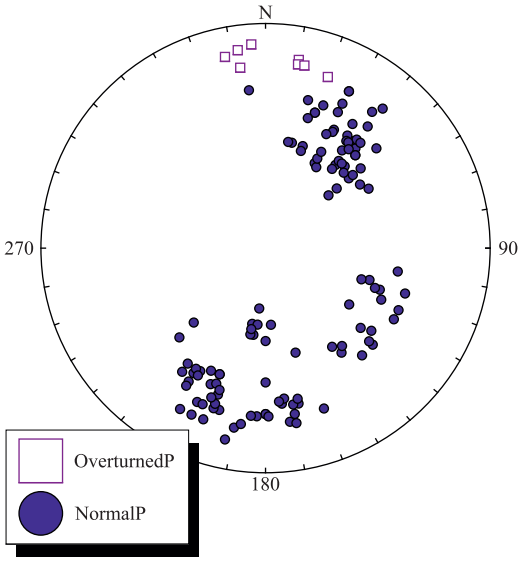

Fig. 3. An example stereonet of planar data categorized as either normal or overturned.

```
(* plot the data *)
SimpleEqualAreaPlot[data, "P", 0.02, {Black,"FCircle"}]
```

2.2. Orientation matrix and distribution classification

As it is standard practice in the analysis of oriented data the eigenvalues and eigenvectors of the orientation matrix provide a good summary of oriented data and permit classification. The orientation matrix is calculated by pre-multiplying the matrix of direction cosines by its transpose (Fisher et al., 1987, p. 33). Given a set of direction cosine data the orientation matrix is

$$T = \begin{pmatrix} \sum x_i^2 & \sum x_i y_i & \sum x_i z_i \\ \sum x_i y_i & \sum y_i^2 & \sum y_i z_i \\ \sum x_i z_i & \sum y_i z_i & \sum z_i^2 \end{pmatrix}$$

The eigenvalues and corresponding eigenvectors of T are denoted by τ_1,τ_2,τ_3 and u_1,u_2,u_3 respectively where $0 \le \tau_1 \le \tau_2 \le \tau_3$. If the normalized eigenvalues of the orientation matrix are given by $\tau_1 = \tau_1/n$ etc. then the shape of the distribution is described by

$$\gamma = \frac{\log(\tau_3/\tau_2)}{\log(\tau_2/\tau_1)}$$

where γ close to 0 is a girdle distribution and γ near 1 is mixed and $\gamma >> 1$ is a uniaxial cluster distribution. The strength or intensity of the distribution is described by

$$\zeta = \log(\tau_3/\tau_1)$$

where values close to 0 indicate weak distributions and strong distributions occur for ζ greater than around 3

In the case of a uniaxial distribution τ_3 is considerably larger than the other two eigenvalues and the eigenvector u_3 provides a good estimate of the average orientation. In the case of a girdle distribution τ_3 and τ_2 are larger than τ_1 and u_1 is a good estimate for the pole to the best fit great circle.

For convenience a method named AnalyseSGData is provided which takes a single dataset returned from ImportSG as its first argument and the second argument is either "T" for text output or "G" for graphical output. Further arguments control the graphical output. The third argument controls the symbol used for data, the fourth argument controls the eigenvector symbol and the final argument specifies the colour of the great circle arcs. Textual output consists of the normalized eigenvalues, the trend and plunge of the eigenvectors, the shape and strength parameters. Example code:Click here to enter text.

```
(* select the directory with the data *)
SetDirectory["C:\\Users\\km\\Dropbox\\research
papers\\Conical Folding Mathematica\\Data"]
(* import data from csv file *)
data=ImportSG["inner_anticline.csv"];
(* check the number of datasets *)
Length[data]
2Click here to enter text.
(* analyse each dataset separately and get textual output *)
AnalyseSGData[data[1],"T"]
{{0.00249152,0.0348249,0.962684},{{308.666,70.0896},
{185.671,11.1581},{92.3696,16.2737}},1.25856,5.95683}
AnalyseSGData[data[2],"T"]
{{0.0618874,0.453435,0.484678},{{20.4175,22.6605},
{149.174,56.3001},{279.942,23.5327}},0.0334578,2.05817}
(* generate graphical output *)
```

```
AnalyseSGData[ data[1], "G", {Black, "Square"}, {Black,
"OCircle"}, Black]
AnalyseSGData[ data[2], "G", {Black, "Square"}, {Black,
"OCircle"}, Black]
```

The associated graphical output is shown in Fig. 4. The eigenvectors are marked on the resulting plot and labelled by their corresponding eigenvalue (to).

2.3. Fitting a cone

The method implemented for fitting a cone is that of Fisher et al. (1987) pp. 140-143, which is based on Mardia and Gadsden (1977) and seeks to minimize the angular distance between points distributed on the sphere and a small circle, i.e. the cone. Let the cone axis have direction cosines $\lambda=(\lambda,\mu,\nu)$ and angular distance from a point on the cone to the axis is ψ. The equation of directions/points (x,y,z) on the cone is

$$x\lambda+y\mu+z\nu=\cos\psi$$

Let the j^{th} estimate of λ be λ_j and that of ψ be ψ_j. The iterative algorithm proceeds as follows:

(1) Take u_3 to be an initial guess for (λ,μ,ν), i.e. $\lambda_0=u_3$.
(2) Calculate ψ_j from

$$\tan\psi_j=\frac{\sum_{i=1}^{n}\sqrt{1-(X_i\lambda_{j-1})^2}}{\sum_{i=1}^{n}X_i\lambda_{j-1}}$$

(3) Calculate the following vectors:

$$X_i=\frac{(X_i\lambda_{j-1})X_i-\lambda_{j-1}}{\sqrt{1-(X_i\lambda_{j-1})^2}},i=1\text{n}$$

$$Y=\cos\psi_j\sum_{i=1}^{n}X_i-\sin\psi_j\sum_{i=1}^{n}X_i$$

$$\lambda_j=\frac{Y}{\sqrt{YY}}$$

(4) Repeat steps 2 and 3 until the difference between the current and previous estimates for λ and ψ is acceptably small.

The algorithm works well when all the target data occupies a single hemisphere but may fail otherwise. This is fixed by applying a rotation to the data such that the first eigenvector (u_3) is rotated into parallelism with the z-axis. The analysis is then

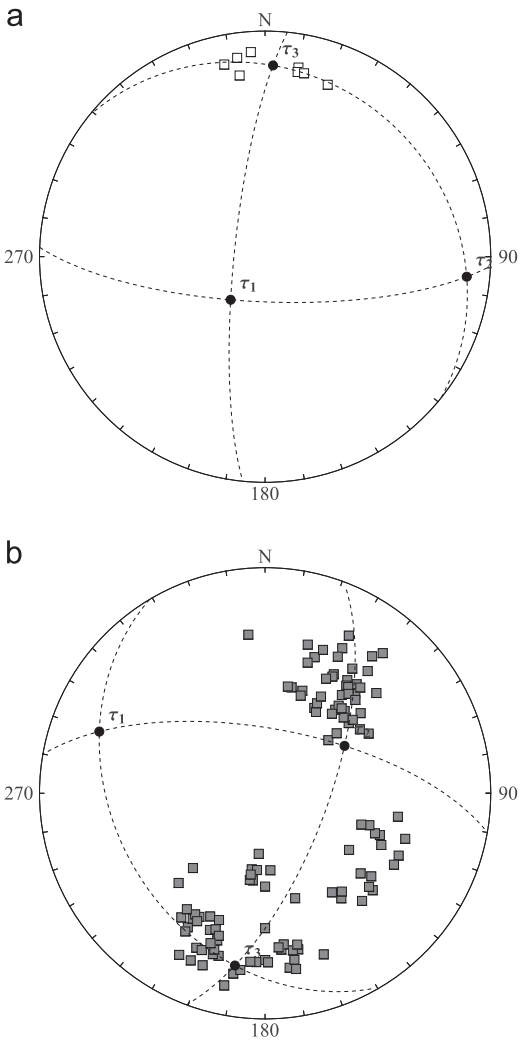

Fig. 4. (a) Eigen analysis of cluster data, note that the eigenvector corresponding to the largest eigenvalue (u_3) parallels the average direction. (b) In this case the eigenvector corresponding to the lowest eigenvalue parallels the pole to the best fit great circle.

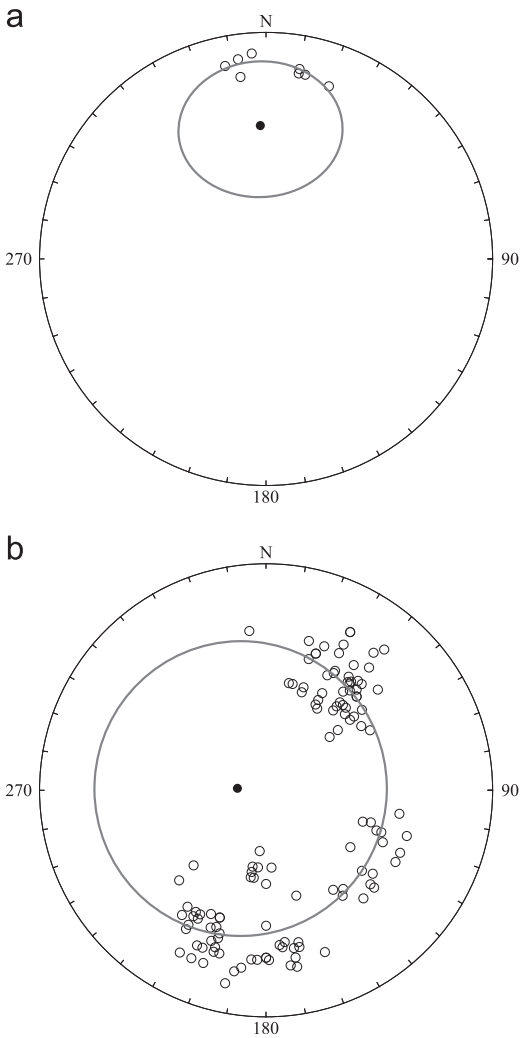

Fig. 5. Best fit cones using the algorithm described.

carried out as described above except that the fitted cone axis is rotated back to the correct orientation.

The algorithm works well when the apical angle is less than approximately 45°. For larger apical angles the algorithm may fail. This is due to exclusively using the third eigenvector as an initial guess for the cone axis. If the apical angle is less than 45° then u_3 takes an orientation close to the cone axis. On the other hand if the apical axis is greater than 45° then it may be one of the other eigenvectors which is close to the cone axis and should be used as an initial guess. Thus a parameter is provided which allows the user to specify the eigenvector to use as an initial guess. The AnalyseSGData method of the previous section allows visual inspection to deduce the correct initial eigenvector to be selected (see Section 2.4 for examples).

Cone fitting is facilitated by the method FitConeSG which takes a single dataset returned from ImportSG as its first argument and the second argument is either "T" for text output or "G" for vectorial graphical output. The third argument controls the symbol used for data, the fourth argument controls the cone axis symbol and the fifth argument specifies the colour of the cone curve. The final argument must be one of 1, 2 or 3 and specifies the eigenvector to be used as an initial guess, by default it takes the value 3. The textual output returns the trend and plunge of the cone axis and the apical angle. After importing the data from the file "inner_anticline.csv" as was done in the previous example:Click here to enter text.

```
(* analyse each dataset separately and get textual output *)
FitConeSG[data [1], "T"]
{{357.535, 40.7466}, 26.9394}
FitConeSG[data [2], "T"]
{{273.907, 79.7289}, 54.54}
(* generate graphical output *)
FitConeSG[data [1], "G", {Black, "Circle"}, {Black, "FCircle"}, Gray]
FitConeSG[data [2], "G", {Black, "Circle"}, {Black, "FCircle"}, Gray]
```

The corresponding graphics are illustrated in Fig. 5. We give a synthesis of the possible commands in Table 1.

2.4. Generating synthetic data and testing cone fitting

For the purposes of testing the cone fitting algorithm a method called GenSGData was developed to generate synthetic conically arranged data. Its first argument is the trend and plunge of the cone axis, the second argument is the apical angle, the third argument specifies the standard deviation around the apical angle and the final argument specifies the number of data to generate. The method works by generating a unit vector **v** randomly oriented in the *xy*-plane and then rotating a unit vector parallel to the z-axis around **v** by an angle selected from a normal distribution with mean equal to the apical angle and the specified standard deviation. Finally the cone is rotated in parallel with the desired cone axis.

To analyse the data produced by GenSGData it is necessary to place it in a csv file confirming to the format specified earlier. This process is simplified by the ExportSGData method which takes as its first argument the trend/plunge data generated by GenSGData, the second argument is the name of the csv file and the last argument is the category.

Two example datasets presented in Fig. 6 indicate the robustness of the method and code.

Example 1 (. see Fig. 6a and b):

```
(* generate data with cone axis trending 054 and plunging 60, apical angle 70, standard deviation of 5 and 50 points *)
datatest = GenSGData[{54, 60}, 70, 5, 50];
(* Export the data to the file "test1.csv" and category "Test 1" *)
ExportSGData[datatest, "test1.csv", "Test1"]
(* Import the data from the file *)
data = ImportSG["test1.csv", "DDD"];
```

Table 1
Synthesis of every argument necessary for conical best fit.

Method	Parameters	Description
ImportSG	Filename	Name of file to be imported
	Format	Data format, either righthand rule "RHR" or dip/dip direction "DDD"
EqualAreaPlot	Data	Data to be plotted (output from ImportSG)
	Pointrad	Size of points plotted (default value 0.02)
	Igoptions	Specify colour/shape of each dataset in a list e.g. {{Blue, OCircle},{Red,FCircle}}
	Legend	True/False display a legend or not
SimpleEqualAreaPlot	Data	Data to plot e.g. {{350,25},{120.56},{249,22}}
	Type	Either "P" or "L" to specify planar or linear data
	Pointrad	Size of points plotted (default value 0.02)
	Igoptions	Specify colour/shape of the plotted points e.g. {Blue, OCircle}
	Labels	An optional ordered list of labels to be placed near each point
AnalyseSGData	Data	A single dataset returned from ImportSG
	Out	"T" for textual output and "G" for graphical output, default value"T"
	Goptdata	Specify colour/shape of the plotted points e.g. {Blue, OCircle}
	Gopteig	Specify colour/shape of the eigenvector directions e.g. {Blue, OCircle}
	Arccolor	Specify colour of arcs e.g. Black
FitConeSG	Data	A single dataset returned from ImportSG
	Out	"T" for textual output and "G" for graphical output, default value"T"
	Goptdata	Specify colour/shape of the plotted points e.g. {Blue, OCircle}
	Gopteig	Specify colour/shape of the cone axis e.g. {Blue, OCircle}
	Arccolor	Specify colour of best fit cone trace e.g. Black
	Eigindex	Specify the index of the eigenvector to use as a seed in the algorithm (1,2 or 3)
GenSGData	Coneaxis	Trend/plunge of the cone axis e.g. {54,60}
	Apicalangle	Apical angle of the cone e.g. 30
	Stddev	Controls the level of dispersion around the apical angle
	n	Number of data to generate
ExportSGData	Data	A dataset created by GenSGData
	File	File in which to store the data
	Category	Specify a category for the data

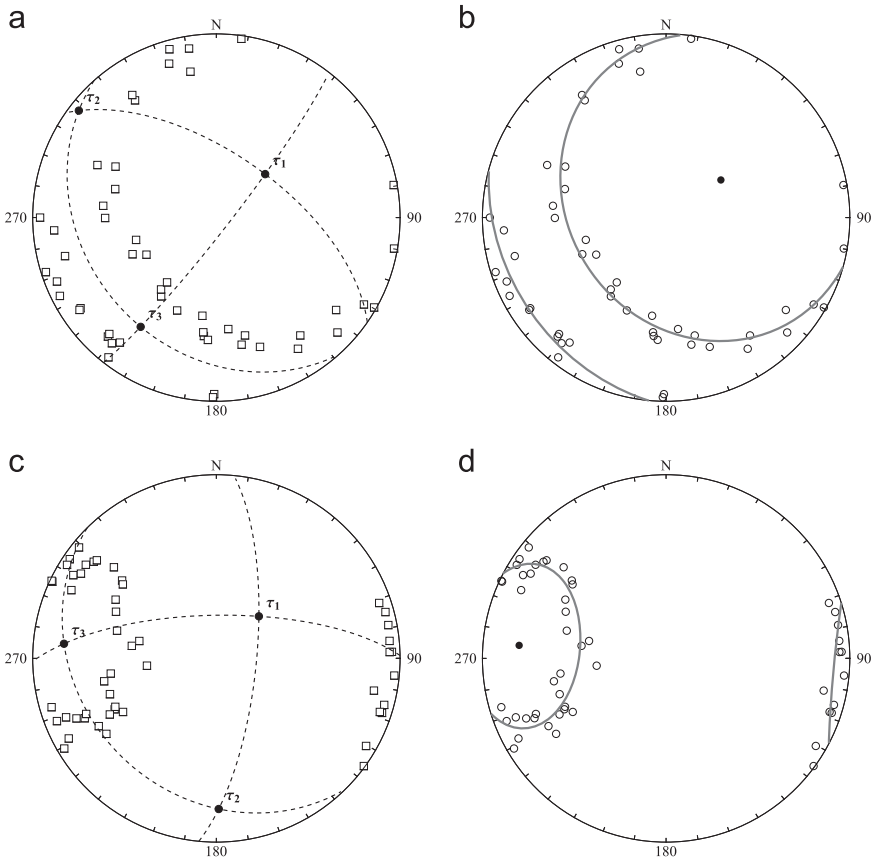

Fig. 6. Synthetically generated data demonstrating the robustness of the algorithm against large apical angle and also data which is not all contained in the same hemisphere. (a) In this case the apical angle is large and the first eigenvector must be used as an initial guess. (b) In this case the apical angle is moderate and the third eigenvector is used as an initial guess.

```
(* check which eigenvalue to use see Fig. 6 a *)
AnalyseSGData[
(1) data[[1]], "G", {Black, "Square"}, {Black, "OCircle"}, Black]
(* fit a cone: textual output *)
FitConeSG[data[1], "T", {Black, "Circle"}, {Black, "FCircle"},
Gray, 1]
{{55.5225, 60.3531}, 71.4319}
(* fit a cone: graphical output see Fig. 6 b *)
FitConeSG[data[1], "G", {Black, "Circle"}, {Black, "FCircle"},
Gray, 1]
```

Example 2. (see Fig. 6c and d):

```
(* generate data with cone axis trending 275 and plunging 20,
apical angle 30, standard deviation of 5 and 50 points *)
datatest = GenSGData[{275, 20}, 30, 5, 50];
(* Export the data to the file "test1.csv" and category "Test
1" *)
ExportSGData[datatest, "test1.csv", "Test1"]
(* Import the data from the file *)
data=ImportSG["test1.csv", "DDD"];
(* check which eigenvalue to use see Fig. 6 c *)
AnalyseSGData[
(1) Data [[1], "G", {Black, "Square"}, {Black, "OCircle"}, Black]
(* fit a cone: textual output *)
FitConeSG[data [1], "T", {Black, "Circle"}, {Black, "FCircle"},
Gray, 3]
{{275.064, 20.7766}, 30.2915}
(* fit a cone: graphical output see Fig. 6 d *)
FitConeSG[data [1], "G", {Black, "Circle"}, {Black, "FCircle"},
Gray, 3]
```

3. A natural example

One of the possible locations of conical folding is in orogens where a phase of deformation is primarily caused by differential rotation around a vertical axis affecting a population of geological surfaces with a variety of initial orientations (Pastor-Galán et al., 2012a) meaning that the orogen shows some degree of curvature in plan view. This plan view curvature is recognized in a large number of ancient and modern orogens (e.g. Weil et al., 2000, 2001; Johnston, 2001; Kaymakci et al., 2003; Weil and Sussman, 2004; Marshak, 2004; Van der Voo, 2004; Rosenbaum and Lister, 2004; Allmendinger et al., 2005; Dupont-Nivet et al., 2005; Johnston and Mazzoli, 2009; Johnston and Gutierrez-Alonso, 2010; Pastor-Galán et al., 2011, 2012b; Pastor-Galán et al., 2013; Rosenbaum et al., 2012; Li et al., 2012; Shaw et al., 2012).

A well known orocline or secondary arc is the Ibero Armorican orocline (Fig. 6), which has been recently defined as a true thick-skinned orocline (Gutiérrez-Alonso et al., 2004; Pastor-Galán et al., 2012b), constraining kinematics and deformation timing (Weil et al., 2001; Gutiérrez-Alonso et al., 2012; Pastor-Galán et al., 2011) which contains in its core the ca. 180° (isoclinally) buckled foreland fold-and-thrust belt of the Carboniferous Variscan orogenic belt, known as the Cantabrian orocline. This curved sector of the orogenic belt is characterized by two different fold sets: (1) one runs parallel to the outcrops of the main thrusts and describes a horseshoe shape concave towards the east, and (2) another is radial to the arc (Julivert and Marcos,

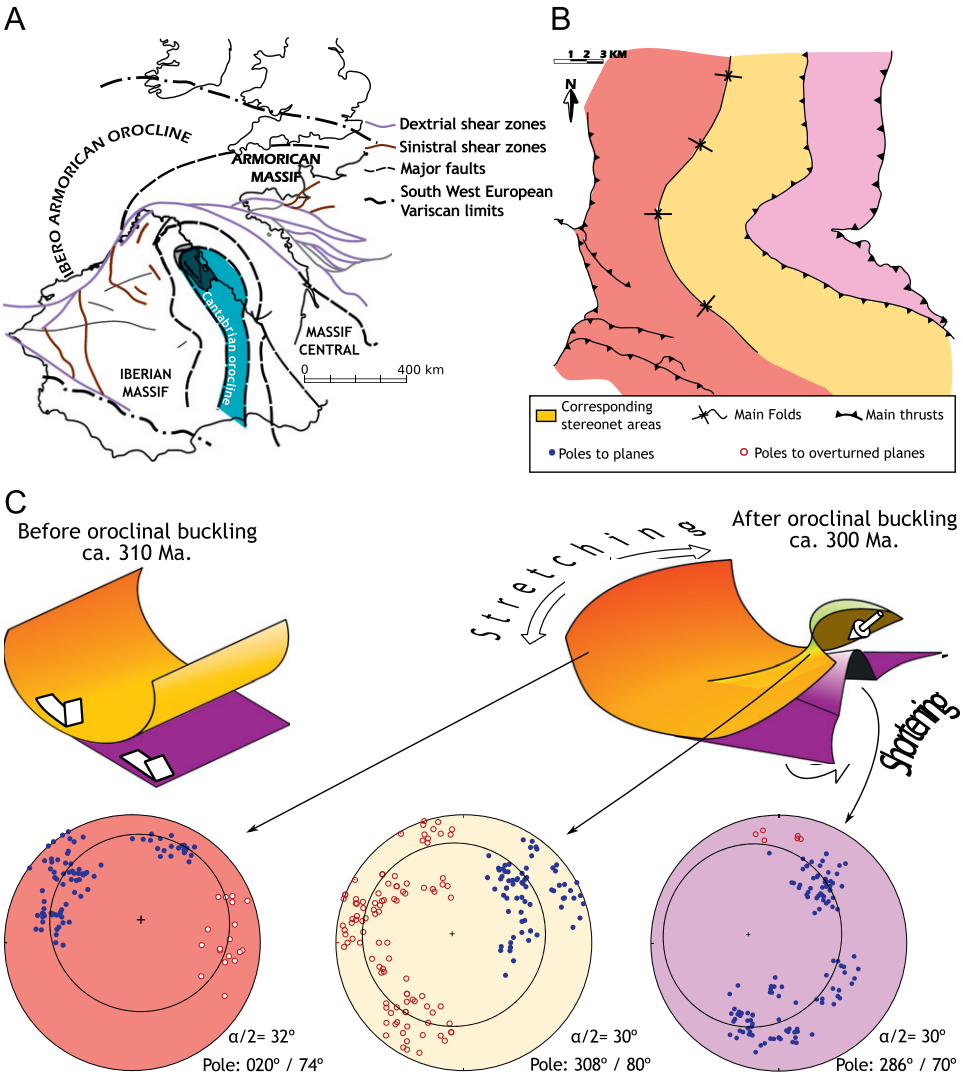

Fig. 7. (a) Situation of the Cantabrian Orocline into the West European Variscides. (b) Studied area showing the mechanism of formation of the Cantabrian Orocline suggested by Pastor-Galán et al. (2012a) and the stereograms obtained with the Mathematica code presented in the different areas of the studied structure.

1973). A detailed geometric study of the fold interference patterns in the Cantabrian Arc revealed the conical nature of the folds belonging to the radial set. These conical folds developed with different geometrical characteristics (semiapical angles and axis attitudes) depending on the initial orientation and geometry of the folded surfaces. They are interpreted to result from a vertical axis rotation during oroclinal buckling of the Variscan Belt in NW Iberia (Fig. 7; Pastor-Galán et al., 2012a).

Data consisting of 578 strike and dip measurements were collected from bedding surfaces of different rock formations (Fig. 7; see Pastor-Galán et al., 2012a for further information) in the Cantabrian Arc. To obtain the best conical fit, folds that have overturned limbs were projected in the lower hemisphere together with the data from the normal limbs.

The geometric study of the fold interference patterns in the Cantabrian Arc revealed the conical nature of the folds belonging to the radial set (Fig. 7) These conical folds developed with different geometrical characteristics depending on the initial orientation and geometry of the folded surfaces. This conical folding is interpreted to result from a vertical axis rotation during oroclinal buckling of the Variscan Belt in NW Iberia (Pastor-Galán et al., 2012a).

4. Conclusions

Due to the lack of available software adequate to do a proper conical fit, we have developed a Mathematica code implementing the Fisher et al. (1987) pp. 140–143, based on Mardia and Gadsden (1977), for least-squares cone fitting. With this code it is possible to obtain semi-apical angles of the cones, orientation of fold axes and errors. Additionally, it exports the stereographic projection as vector graphics format (.pdf files) facilitating the edition of figures to be published.

We have tested the code firstly with synthetic datasets in order to notice the robustness of the method and code. After that, we tested the method and code with a complex geometric natural example from NW Iberia. Both tests indicate that the method used is confident and the robustness of the code to obtain the best conical fit using stereographic projection.

Acknowledgements

This paper is part of the IGCP Project from UNESCO No. 574: Bending and Bent Orogens, and Continental Ribbons. Financial

support was supplied by Research Project ODRE II (“Oroclines and Delamination: Relations and Effects”) CGL2009-1367 from the Spanish Ministry of Science and Innovation. DPG is also granted by an ACPI fellowship from the Junta de Castilla and León co-funded by the European Union. We want to thank two anonymous reviewers that helped to improve the paper. We also thank Rod Holcombe for a free license of his software GEOrient (http://www.holcombe.net.au/software/rodh_software_georient.htm).

Appendix A. Supporting information

Supplementary data associated with this article can be found in the online version at http://dx.doi.org/10.1016/j.cageo.2013.01.005.

References

Allmendinger, R.W., Cardozo, N., Fisher, D.M., 2012. Structural Geology Algorithms: Vectors and Tensors. Cambridge University Press.
Allmendinger, R.W., Smalley, R., Bevis, M., Caprio, H., Brooks, B., 2005. Bending the Bolivian orocline in real time. Geology 33, 905–908.
Alsop, G.I., Carreras, J., 2007. The structural evolution of sheath folds: a case study from Cap de Creus. Journal of Structural Geology 29, 1915–1930.
Cardozo, N., Allmendinger, R.W., 2013. Spherical projections with OSXStereonet. Computers & Geosciences 51, 193–205.
Cruden, D.M., Charlesworth, H.A.K., 1972. Observations on the numerical determination of axes of cylindrical and conical folds. Geological Society of America Bulletin 83, 2019.
Cummins, W.A., 1966. Conical folding and sedimentary lineations. Geological Magazine 103, 197–203.
Dupont-Nivet, G., Vasiliev, I., Langereis, C.G., Krijgsman, W., Panaiotu, C., 2005. Neogene tectonic evolution of the southern and eastern Carpathians constrained by paleomagnetism. Earth and Planetary Science Letters 236, 374–387.
Fisher, N.I., Lewis, T., Embleton, B.J.J., 1987. Statistical Analysis of Spherical Data. Cambridge University Press.
Gray, N., Geiser, P., Geiser, J., 1980. On the least-squares fit of small and great circles to spherically projected orientation data. Mathematical Geology 12, 173–184.
Grohmann, C.H., Campanha, G.A., 2010. OpenStereo: Open Source, Cross-Platform Software for Structural Geology Analysis. AGU Fall Meeting abstracts.
Groshong, R.H., 2008. 3-D Structural Geology: A Practical Guide to Quantitative Surface and Subsurface Map Interpretation. Springer.
Gutiérrez-Alonso, G., Fernández-Suárez, J., Weil, A.B., 2004. Orocline triggered lithospheric delamination. In: Weil, A.B., Sussman, A. (Eds.), Paleomagnetic and Structural Analysis of Orogenic Curvature, Special Paper. Geological Society of America, Boulder, pp. 121–131.
Gutiérrez-Alonso, G., Johnston, S.T., Weil, A.B., Pastor-Galán, D., Fernández-Suárez, J., 2012. Buckling an orogen: The Cantabrian Orocline. GSA Today 22, 4–9 ç.
Hanebergs, B. Matematica for Geology. 〈http://www.haneberg.com/Mathematica.html〉.
Johnston, S.T., 2001. The Great Alaskan Terrane Wreck: reconciliation of paleomagnetic and geological data in the northern Cordillera. Earth and Planetary Science Letters 193, 259–272.
Johnston, S.T., Gutierrez-Alonso, G., 2010. The North American Cordillera and West European Variscides: contrasting interpretations of similar mountain systems. Gondwana Research 17, 516–525.
Johnston, S.T., Mazzoli, S., 2009. The Calabrian Orocline: Buckling of a Previously More Linear Orogen. Geological Society. Special Publications, London 327, 113–125.
Julivert, M., Marcos, A., 1973. Superimposed folding under flexural conditions in the Cantabrian Zone (Hercynian Cordillera, northwest Spain). American Journal of Science. 273, 353–375.
Kaymakci, N., Duermeijer, C.E., Langereis, C., White, S.H., Van Dijk, P.M., 2003. Palaeomagnetic evolution of the Cankiri Basin (central Anatolia, Turkey): implications for oroclinal bending due to indentation. Geological Magazine 140, 343–355.
Kelker, D., Langenberg, C., 1982. A mathematical model for orientation data from macroscopic conical folds. Mathematical Geology 14, 289–307.
Kelker, D., Langenberg, C.W., 1976. Mathematical-model for orientation data from macroscopic cylindrical folds. Mathematical Geology 8, 549–559.
Kelker, D., Langenberg, C.W., 1988. Statistical classification of macroscopic folds as cylindrical, circular conical, or elliptical conical. Mathematical Geology 20, 717–730.
Kelker, D., Langenberg, C., 1987. A mathematical model for orientation data from macroscopic elliptical conical folds. Mathematical Geology 19, 729–743.
Keppie, D., Keppie, J.D., Murphy, B., 2002. Saddle reef auriferous veins in a conical fold termination (Oldham anticline, Meguma terrane, Nova Scotia, Canada): reconciliation of structure and age data. Canadian Journal of Earth Sciences 39, 53–63.
Li, P., Rosenbaum, G., Donchak, P.J.T., 2012. Structural evolution of the Texas Orocline, eastern Australia. Gondwana Research 22 (1), 279–289.
Mandujano V., J.J., Keppie M., J.D, 2006. Cylindrical and conical fold geometries in the cantarell structure, Southern Gulf of Mexico: implications for hydrocarbon exploration. Journal of Petroleum Geology 29, 215–226.
Mardia, K.V., Gadsden, R.J., 1977. A circle of best fit for spherical data and areas of volcanism. Applied Statistics 26, 238–245.
Marshak, S., 2004. Salients, recesses, arcs, oroclines, and sytaxes – a reviewof ideas concerning the formation of map-view curves in fold-and-thrust belts. In: Thrust Tectonics and Hydrocarbon Systems: AAPG Memoir 82. pp. 131–156.
Mookerjee, M. Geological Programs for Mathematica program suite 〈http://www.sonoma.edu/users/m/mookerje/ProgramPage.htm〉.
Mulchrone, K.F., 1991. The interpretation of fold axial data from regions of polyphase folding. Journal of Structural Geology 13, 275–280.
Nicol, A., 1993. Conical folds produced by dome and basin fold interference and their application to determining strain: examples from North Canterbury, New Zealand. Journal of Structural Geology 15, 785–792.
Pastor-Galán, D., Gutiérrez-Alonso, G., Mulchrone, K.F., Huerta, P., 2012a. Conical folding in the core of an orocline. A geometric analysis from the Cantabrian Arc (Variscan Belt of NW Iberia). Journal of Structural Geology 39, 210–223.
Pastor-Galán, D., Gutiérrez-Alonso, G., Murphy, J.B., Fernández-Suárez, J., Hofmann, M., Linnemann, U., 2013. Provenance analysis of the Paleozoic sequences of the northern Gondwana margin in NW Iberia: passive margin to Variscan collision and orocline development. Gondwana Research 23 (3), 1089–1103.
Pastor-Galán, D., Gutiérrez-Alonso, G., Weil, A.B., 2011. Orocline timing through joint analysis: insights from the Ibero-Armorican Arc. Tectonophysics 507, 31–46.
Pastor-Galán, D., Gutiérrez-Alonso, G., Zulauf, G., Zanella, F., 2012b. Analogue modeling of lithospheric-scale orocline buckling: constraints on the evolution of the Iberian-Armorican Arc. Geological Society of America Bulletin 124, 1293–1309.
Pueyo, E.L., Pares, J.M., Millan, H., Pocovi, A., 2003. Conical folds and apparent rotations in paleomagnetism (a case study in the Southern Pyrenees). Tectonophysics 362, 345–366.
Ragan, D.M., 2009. Structural Geology: An Introduction to Geometrical Techniques. Cambridge University Press.
Ramsay, J.G., 1962. Interference Patterns Produced by the Superposition of Folds of Similar Type. The Journal of Geology 70, 466–481.
Ramsay, J.G., 1967. Folding and Fracturing of Rocks. McGraw-Hill, New York.
Ramsay, J.G., Huber, M.I., 1987. 1st ed.The Techniques of Modern Structural Geology, Volume 2. Academic Press, Folds and Fractures.
Röller, K., Trepmann, C., 2008. Stereo32 Version 1.01. 〈http://www.ruhr-uni-bochum.de/hardrock/downloads.htm〉.
Rivest, L., 2008. Some linear model techniques for analyzing small-circle spherical data. Canadian Journal of Statistics 27, 623–638.
Rosenbaum, G., Li, P., Rubatto, D., 2012. The contorted New England Orogen (eastern Australia): New evidence from U-Pb geochronology of early Permian granitoids. Tectonics 31, 14.
Rosenbaum, G., Lister, G.S., 2004. Formation of arcuate orogenic belts in the western Mediterranean region. Geological Society of America Special Papers 383, 41–56.
Shaw, J., Johnston, S.T., Gutiérrez-Alonso, G., Weil, A.B., 2012. Oroclines of the Variscan orogen of Iberia: paleocurrent analysis and paleogeographic implications. Earth and Planetary Science Letters 329–330, 60–70.
Stockmal, G.S., Spang, J.H., 1982. A method for the distinction of circular conical from cylindrical folds. Canadian Journal of Earth Sciences 19, 1101–1105.
Van der Voo, R., 2004. Paleomagnetism, oroclines, and growth of the continental crust. GSA Today 14, 4–11.
Venkitasubramanyan, C.S., 1971. Least-squares analysis of fabric data: a note on conical, cylindroidal and near-cylindroidal folds. Canadian Journal of Earth Sciences 8, 694–697.
Webb, B.C., Lawrence, D.J.D., 1986. Conical fold terminations in the bannisdale slates of the English Lake district. Journal of Structural Geology 8, 79–86.
Weil, A.B., Gutiérrez-Alonso, G., Wicks, D., 2013. Investigating the kinematics of local thrust sheet rotation in the limb of an orocline: a paleomagnetic and structural analysis of the Esla Tectonic Unit, Cantabrian-Asturian Arc NW Iberia. International Journal of Earth Sciences 102 (1), 43–60.
Weil, A.B., Sussman, A.J., 2004. Classifying curved orogens based on timing relationships between structural development and vertical-axis rotations. In: Sussman, A.J., Weil, A.B. (Eds.), Orogenic Curvature: Integrating Paleomagnetic and Structural Analyses. Geological Society of America, pp. 1–16.
Weil, A.B., van der Voo, R., van der Pluijm, B.A., 2001. Oroclinal bending and evidence against the Pangea megashear: The Cantabria-Asturias arc (northern Spain). Geology 29, 991–994.
Weil, A.B., Van der Voo, R., van der Pluijm, B.A., Pares, J.M., 2000. The formation of an orocline by multiphase deformation: a paleomagnetic investigation of the Cantabria-Asturias Arc (northern Spain). Journal of Structural Geology 22, 735–756.
Wilson, G., 1967. The geometry of cylindrical and conical folds. Proceedings of the Geologists' Association 78, 179–209, IN11.